Shorter latencies for motion trajectories than for flashes in population responses of cat primary visual cortex

Dirk Jancke[1,2], Wolfram Erlhagen[1,3], Gregor Schöner[1] and Hubert R. Dinse[1]

[1] *Institut für Neuroinformatik ND 04, Theoretische Biologie, Ruhr-Universität Bochum, D-44780 Bochum, Germany*
[2] *Lehrstuhl für Allgemeine Zoologie und Neurobiologie ND 7, Ruhr-Universität Bochum, D-44780 Bochum, Germany*
[3] *Departamento de Matemática para C&T, Universidade do Minho, P-4800-058-Guimarães, Portugal*

Psychophysical evidence in humans indicates that localization is different for stationary flashed and coherently moving objects. To address how the primary visual cortex represents object position we used a population approach that pools spiking activity of many neurones in cat area 17. In response to flashed stationary squares (0.4 deg) we obtained localized activity distributions in visual field coordinates, which we referred to as profiles across a 'population receptive field' (PRF). We here show how motion trajectories can be derived from activity across the PRF and how the representation of moving and flashed stimuli differs in position. We found that motion was represented by peaks of population activity that followed the stimulus with a speed-dependent lag. However, time-to-peak latencies were shorter by ∼16 ms compared to the population responses to stationary flashes. In addition, motion representation showed a directional bias, as latencies were more reduced for peripheral-to-central motion compared to the opposite direction. We suggest that a moving stimulus provides 'preactivation' that allows more rapid processing than for a single flash event.

(Received 28 November 2003; accepted after revision 19 February 2004; first published online 20 February 2004)
Corresponding author D. Jancke: Lehrstuhl für Allgemeine Zoologie und Neurobiologie, ND 7, Ruhr-Universität Bochum, D-44780 Bochum, Germany. Email: jancke@neurobiologie.ruhr-uni-bochum.de

It takes some tens of milliseconds for visual information to reach the cortex. During that time, an approaching object might have moved several meters. Inevitably, mislocalization results unless compensational processes counterbalance for neural processing times. In fact, anticipatory mechanisms have been reported to occur already at the level of retinal ganglion cells (Berry *et al.* 1999). Psychophysically, a moving and a flashed stimulus presented aligned are perceived as being displaced. Surprisingly, the moving stimulus appears ahead of the flash (Hazelhoff & Wiersma, 1924). One explanation for this 'flash-lag' effect is that the visual system is predictive by extrapolating the position of a moving stimulus into the future (Nijhawan, 1994). Alternatively, the 'latency difference' model assumes that the visual system processes moving objects 'on-line' but more rapidly than flashed objects (Purushothaman *et al.* 1999; Kirschfeld & Kammer, 1999; Whitney *et al.* 2000; for review and other explanations see Krekelberg & Lappe, 2001). In none of those studies, however, were neurophysiological correlates examined.

In order to measure neurophysiological representations of flashed or moving stimuli we applied a population approach in the visual cortex that extracts the 'quantity' position from highly overlapping receptive fields (RFs) of many neurones. Their joint activity in response to a fixed set of stimuli was pooled, resulting in fine-scaled distributions of population activity both in visual space and time. Our concept is a straightforward consequence of the observation that a large number of broadly tuned neurones are activated, after even the simplest form of sensory stimulation or motor output. In addition, under natural viewing conditions stimuli are arbitrarily distributed across many RFs with highly diverse spatio-temporal properties (Szulborski & Palmer, 1990; Gegenfurtner & Hawken, 1996; Fitzpatrick, 2000; Dinse & Jancke, 2001*a*,*b*; for a similar approach in the somatosensory system see Nicolelis *et al.* 1998).

We have previously demonstrated that the population approach can provide insight into neural interactions in response to small flashes presented with distances much less than average RF sizes (Jancke *et al.* 1999), and into mechanisms of multidimensional coding (Jancke, 2000). Here we used this technique to study how motion trajectories are presented at the level of primary visual cortex and how the representation of moving stimuli

 DOI: 10.1113/jphysiol.2003.058941

deviates from that of single flashes (Jancke *et al.* 1996). We analysed population activity in response to small squares of light (0.4 deg) that were flashed or moved at different speeds and directions.

We show that in cat area 17 small moving stimuli are represented as propagating peaks of population activity. When compared to the representation of a flash, we found a significant reduction in time-to-peak latencies of the population responses. Reduced neural latencies might contribute to the perceived positional lead of a moving stimulus compared to a flash, as shown psychophysically in humans.

Methods

Animals and preparation

Extracellular recordings from a total of 178 cells were made in the central visual field representation of cat area 17. Neurones of the left hemisphere of anaesthetized cats were recorded as previously described (Jancke *et al.* 1999). Twenty adult animals of both sexes were used. Animals were initially anaesthetized with Ketanest (15 mg (kg body weight)$^{-1}$, I.M., Parke-Davis) and Rompun (1 mg kg^{-1}, I.M., Bayer, Germany). Additionally, Atropin (0.1 mg kg^{-1}, S.C., Braun, Germany) was given. During surgery and recording, anaesthesia was maintained by artificial respiration with a mixture of 75% N_2O and 25% O_2, and by application of sodium pentobarbital (Nembutal, 3 mg kg^{-1} h^{-1}, I.V., Ceva, Germany). Neuromuscular block was established by continuous infusions of gallamine triethiodide (2 mg kg^{-1}, I.V. bolus, 2 mg kg^{-1} h^{-1}, I.V., Sigma). In addition 5% glucose in physiological Ringer solution was continuously infused (3 ml h^{-1}, Braun, Germany). Heart rate, intratracheal pressure, expired CO_2, body temperature, and EEG were controlled during the entire experiment. Respiration was adjusted for an end-tidal CO_2 between 3.5 and 4.0%. Contact lenses with artificial pupils were used to cover the eyes. Pupils were dilated by atropine (5 mg ml^{-1}), and nictitating membranes retracted by noradrenaline (norepinephrine; Neosynephrin-POS, 50 mg ml^{-1}, Ursapharm, Germany). Treatment of all animals was within the regulations of the National Institution of Health Guide and Care for Use of Laboratory Animals (Rev. 1987). At the end of the experiments, animals were killed with an overdose of sodium pentobarbital. All experiments were approved by the German Animal Care and Use Committee.

Recording and stimulation

Stimuli were displayed on a PC-controlled 21-inch monitor (120 Hz, non-interlaced) positioned at a distance of 114 cm from the animal. Luminance of stimulation was 0.9 cd m^{-2}, background luminance was 0.002 cd m^{-2}. Stimuli were repeated 32 times in pseudo-random order and presented to the contralateral eye. Stimuli were presented within a fixed reference frame, irrespective of the receptive field (RF) location of the individual neurones (non-RF-centred approach illustrated in Fig. 1*A*). To control for eye drift, RF locations were repeatedly measured during each recording session. Seven flashed squares of light (0.4 deg) were used to sample 2.8 deg of visual space (Fig. 1*A* and *B*). Additionally, squares were moved horizontally either centro-peripherally or in the opposite direction (Fig. 1*C*). Smooth trajectories were generated by varying the stimulus shift per video frame resulting in different speeds (4.5, 8.8, 15.1, 38.4 deg s^{-1}, length of trajectory was 9.2 deg).

We pooled 178 single cell responses whose receptive fields (RFs) densely covered the central visual field representation of cat area 17 (Fig. 1*A*). Our approach enables us (1) to average activity across a neural population with high spatial and temporal resolution, (2) to include cells with different tuning properties, and (3) to measure activity independently of the individual cell's RF location relative to the stimulus (non-centred approach). To depict the population activity of these neurones, two different coding techniques were used (described below).

RF-derived population representations of stimulus position

We first applied a population code consisting of an interpolation procedure in which each cell 'votes' with its firing rate for the centre of the RF. The RF centres were quantitatively assessed for each cell separately by flashing small dots of light (diameter 0.64 deg) in pseudo-random order (20 times) for 25 ms (ISI 1000 ms) on 36 locations of a six by six grid. The resulting RF profiles were smoothed and the RF centre was defined at the location of maximal amplitude (Jancke *et al.* 1999).

In the next step, population representations of the flashed or moved stimuli presented in a fixed reference frame (Fig. 1*B* and *C*) were derived. To this end, each cell's normalized firing rate in response to the stimuli was mapped to each individual RF centre, resulting in a distribution of activity. The responses were then interpolated with a Gaussian (width = 0.6 deg; to correct for uneven sampling, the distribution was divided by the sum of unweighted Gaussians centred on all RF centres). In summary, each neurone contributes to the entire population activity by its firing rate (1 ms time resolution), which is dependent on the location of the RF centre relative to the stimulus.

OLE-derived population representations of stimulus position

As an alternative to this RF-derived procedure we employed an optimal linear estimator (OLE) technique to reconstruct stimulus position from the observed neuronal population activity. This technique, originally developed to estimate a single value of an encoded physical quantity (Salinas & Abbott, 1994), is based on a Bayesian theoretical framework (Dayan & Abbott, 2001). We used an extension of this method (Erlhagen *et al.* 1999; Jancke *et al.* 1999; Jancke, 2000) that enabled us to estimate entire distributions of population activity across visual space.

The method is based on two ideas. First, the population distribution is generated as a linear superposition of a set of basis functions, one such function for each neurone. Each neurone's basis function is multiplied by the current firing rate of the neurone. Second, for the set of seven joint reference stimuli (Fig. 1*B*), a template function for the distribution of population activity was defined as a Gaussian centred at each of the seven stimulus positions. Its width (0.6 deg) in visual space approximately matched the average RF profile of all neurones measured. A systematic variation of the width parameter showed that the reconstruction results did not critically depend on the exact shape of the template distribution. The basis function each neurone contributes was determined so that for the seven reference stimuli the reconstructed population distribution approximated the template functions optimally. For this optimization, mean firing rates within the time interval from 40 to 65 ms after stimulus onset were used. This is the time for which peak responses are observed in the PSTHs. The exact size of the integration window is not critical for the estimation procedure.

To extend the estimation procedure beyond the seven reference stimuli to the moving stimulus condition, the basis function that each neurone contributes was held fixed, but was now multiplied by the firing rate of that neurone in response to a stimulus moving with a particular velocity. The firing rate was determined in 10 ms bins to obtain time-resolved population representations.

Cumulative post-stimulus-time histograms (PSTHs)

Cumulative PSTHs in response to flashed or moving stimuli were obtained by averaging spiking activity across all neurones in time bins of 10 ms. A cell was judged as significantly active when its firing rate was higher than the mean + 2 s.d. of activity revealed in a no-stimulus condition (recording period 2 s).

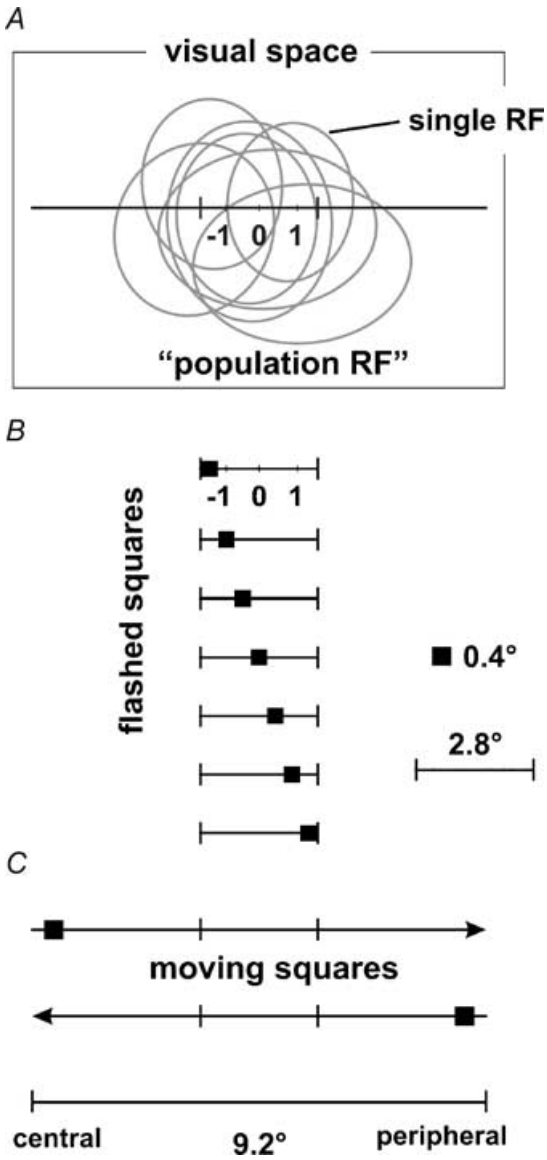

Figure 1. Schematic illustration of the stimulus configurations
A, 178 neurones were recorded within the central visual field representation of cat area 17. Their receptive fields (RFs, a small representative sample is illustrated by grey ellipsoids) densely overlapped within the sampled visual space, which is denoted as 'population receptive field' (PRF). *B*, small squares of light 0.4 × 0.4 deg (depicted in black) were flashed for 25 ms at seven different contiguous horizontal positions across the PRF. Neural responses to each of the squares were used to calculate the individual cell weights by optimal linear estimation (OLE). *C*, squares were moved horizontally at four different speeds (4.5, 8.8, 15.1, 38.4 deg s^{-1}) either centro-peripherally or in opposite direction (arrows). Stimuli started and ended 3.2 deg outside the sampled central visual space resulting in a trajectory of 9.2 deg.

Bootstrap analysis

To investigate how critically the results depend on the current sampling of neurones across visual space, we performed a bootstrap analysis. One thousand iterations were generated, each equal in size to the total number of all cells measured, by drawing neurones (with replacements) from the original data set. For each such 'synthetic' set of neural populations the OLE, representing the population responses to each stimulus, was calculated.

Results

Population representations of moving and flashed stimuli show a spatial offset

We first applied a population approach based on interpolation of many cell responses (Anderson, 1994; Jancke *et al.* 1999; see Berry *et al.* 1999 for a similar approach in the retina). The resulting distributions of activity can be regarded as the profile of a population receptive field (PRF) in which each neurone contributes to the overall activity via its RF location relative to stimulus position. Thus, flashing a stimulus at a specific site will predominantly activate neurones that have their RF centres close to the stimulus whereas neurones further away respond with lower firing rates. In response to a small flashed square, the population representation therefore results in a gradual and well-localized peak of activity centred on the position of the stimulus (Fig. 2, upper row; each frame shows a 10 ms time step).

The lower row in Fig. 2 illustrates the central portion of a motion trajectory of a square moving at 38.4 deg s^{-1}. At flash onset (upper row, time zero), the moving square was located at the same position as the flashed square. Due to neural delay times, cortical population activity for the flash was zero. In contrast, for the moving square, a propagating peak of activity was observed that had been evoked previously since the stimulus trajectory started much earlier outside the PRF. Five time steps later (50–60 ms), the moving stimulus was at a new position, tracked by the peak of population activity with a spatial lag. At that time, activity for the flash reached its maximum but did not change position, thus representing faithfully the initial location of the stimulus. Assuming equal processing times for both stimuli, the population representations should be localized at identical positions. Instead, the activity peaks elicited by the moving square and the flash showed a significant spatial offset, i.e. the moving square was represented ahead of the flash, indicating shorter latencies for motion.

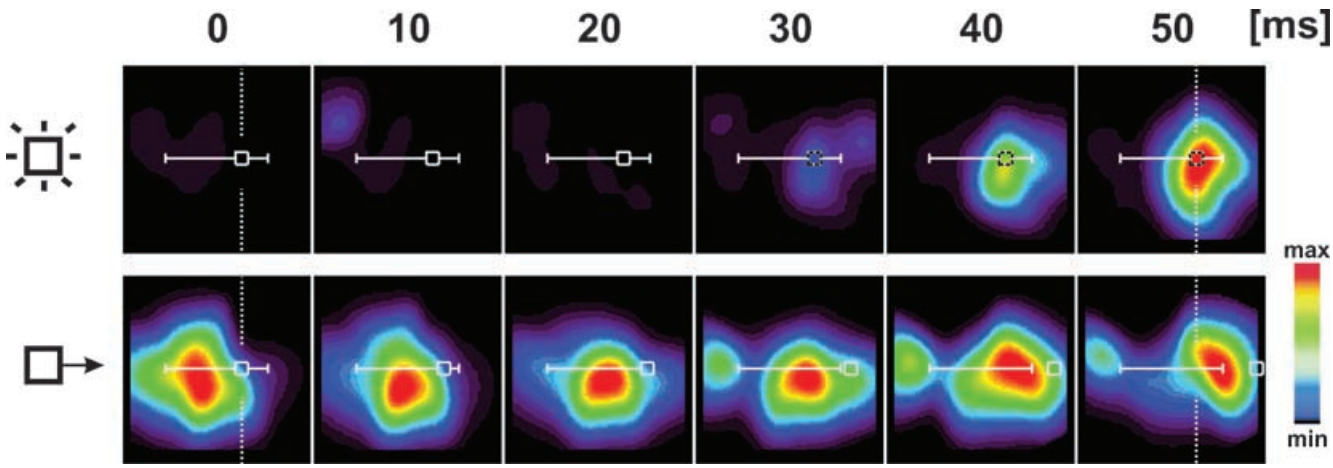

Figure 2. The flash lags: impact of shorter latency for motion compared to a flash on the representation of position

Population representation derived from Gaussian interpolation. Upper row: flashed square (outlined in white; 25 ms on; shown stippled after stimulus off). Lower row: moving square (38.4 deg s^{-1}). To obtain the population representations, individual firing rates were depicted at each neurone's RF centre and interpolated using a two-dimensional Gaussian profile. Frames from left to right show time frames of 10 ms. The sampled space covered 2.8 deg of the central visual field (horizontal white line, see Fig. 1). Colour key indicates level of population activity; data were normalized separately for each stimulus condition. The moving stimulus started 3.2 deg outside the PRF tracked by a peak of population activity that has been evoked a number of time steps before. At time zero stimulus position was identical for the moving and the flashed square (compare vertical pointed lines). During the next time steps activity in response to the flash emerged while the moving peak continued propagating. When activity for the flashed stimulus reached its maximum (50 ms), the moving peak had already passed the mutual flash position due to its faster processing.

Population representations of flashed stimuli

To show raw population data before employing any coding procedure, Fig. 3*A* depicts the temporal evolution of activity in cumulative PSTHs (sum of activity across all neurones) for squares that were flashed at three adjoining positions (as shown in Fig. 3*B*). Firing rates for individual cells were 13–58 spikes s^{-1}, which is within the range typically found for neurones in cat area 17 (Bishop *et al.* 1971; Orban, 1984). Cumulative activity for more peripheral stimulus positions was slightly lower, due to the fact that less RFs were overlapping at the border than within the central part of the sampled space. However, for each stimulus position the number of cells contributing to the cumulative PSTHs was more than half of the entire population, even for the most peripheral stimulus positions (∼90 cells; Fig. 3*C*), demonstrating the dense and homogeneous sampling.

In order to construct the PRF in a well-defined mathematical way, we applied an optimal linear estimator (OLE) (Salinas & Abbott, 1994; Erlhagen *et al.* 1999; Jancke *et al.* 1999; Jancke, 2000) that assigns to each neurone's firing a 'weighting coefficient' calculated by optimizing the contribution of each neurone with respect to its relative RF position. As a result, Fig. 3*B* depicts distributions of population activity with high precision in visual space. For each stimulus position, we observed a homogenous build-up and decay of activity accurately centred on the different stimulus loci. Thus, all seven flashes used were fairly represented by 0.4 deg shifts of activity profiles across the PRF (Fig. 3*D*). The mean time-to-peak latency across all squares was 54 ± 3 ms.

To test how critically the PRF profiles were dependent on the actual sample of neurones, we applied a bootstrap analysis in which the population was repetitively ($n = 1000$) composed by 'drawing' 178 neurones with replacements from the original data set. Figure 3*D* depicts the distributions of activity for all seven squares within the time window of maximal discharge (50–60 ms). The analysis revealed that the OLE procedure guarantees a precise decoding of the actual stimulus positions across the entire sampled visual space. Furthermore, the observed scatter in amplitudes was not significantly dependent on the actual sampling except for a small bias in response to the most central stimulus.

Population representation of moving stimuli

To compare data from flashed stimuli with responses to moving squares we first show cumulative PSTHs for all speeds and for both directions (Fig. 4; blue = centro-peripheral; red = periphero-central). Increasing speeds (top to bottom) evoked increasing amplitudes of the responses. All moving stimuli recruited similar numbers of responding cells (see upper curves), thus the individual cell's firing rates were enhanced with speed. For slow speeds (4.5, 8.8 deg s^{-1}) the PSTHs show a moderate slope of rising and decaying activity as it takes the stimulus longer to pass the PRF than for high speeds. In contrast, higher stimulus speeds (15.1, 38.4 deg s^{-1}) induced more brisk responses and a second peak that occurred when the stimulus had already passed the PRF. Such a 'rebound' response (Camarda *et al.* 1985) has recently been shown to contain information about stimulus orientation at the population level (Jancke, 2000).

Second, to derive stimulus trajectories across the sampled PRF, we again applied the OLE procedure resulting in distributions of activity that unravel each cell's contribution to the current stimulus position. For all speeds and both directions tested, Fig. 5 depicts space–time diagrams of population distributions within the time intervals that revealed significant propagation of activity. The diagrams show coherent peaks of activity tracking each moving stimulus across the PRF. We observed a spatial lag between the current stimulus position and the activity peaks, which was dependent on speed and most evident at high stimulus speeds (see red, blue lines at bottom). The profiles of the PRF showed some variability in response amplitudes and scatter in peak positions. These fluctuations were due to irregularities in cell sampling and of no significance ($P > 0.05$, bootstrap, $n = 1000$; see Supplementary material, available online only). Thus, our approach allows for visualization of propagating activity on a fine spatial scale, resolving shifts of activity peaks in a visual space much smaller than RF sizes. Next, we exploited this outcome to derive latencies from the representation of moving stimuli.

Reduced latencies dependent on motion direction

In order to compare latencies evoked by a single flash with the latencies for moving stimuli, we used the spatial lag method introduced by Bishop *et al.* (1971) for analysis of single cell latencies. This method uses the fact that the time-to-peak of activity depends on stimulus speed: with increasing speeds the stimulus passes longer distances until the discharge peak is reached. However, as our approach produces continuous trajectories rather than only one single discharge peak we modified the original method: for each iteration within a bootstrap analysis, we first determined the time interval within significant propagation of peak activity occurred by calculating linear

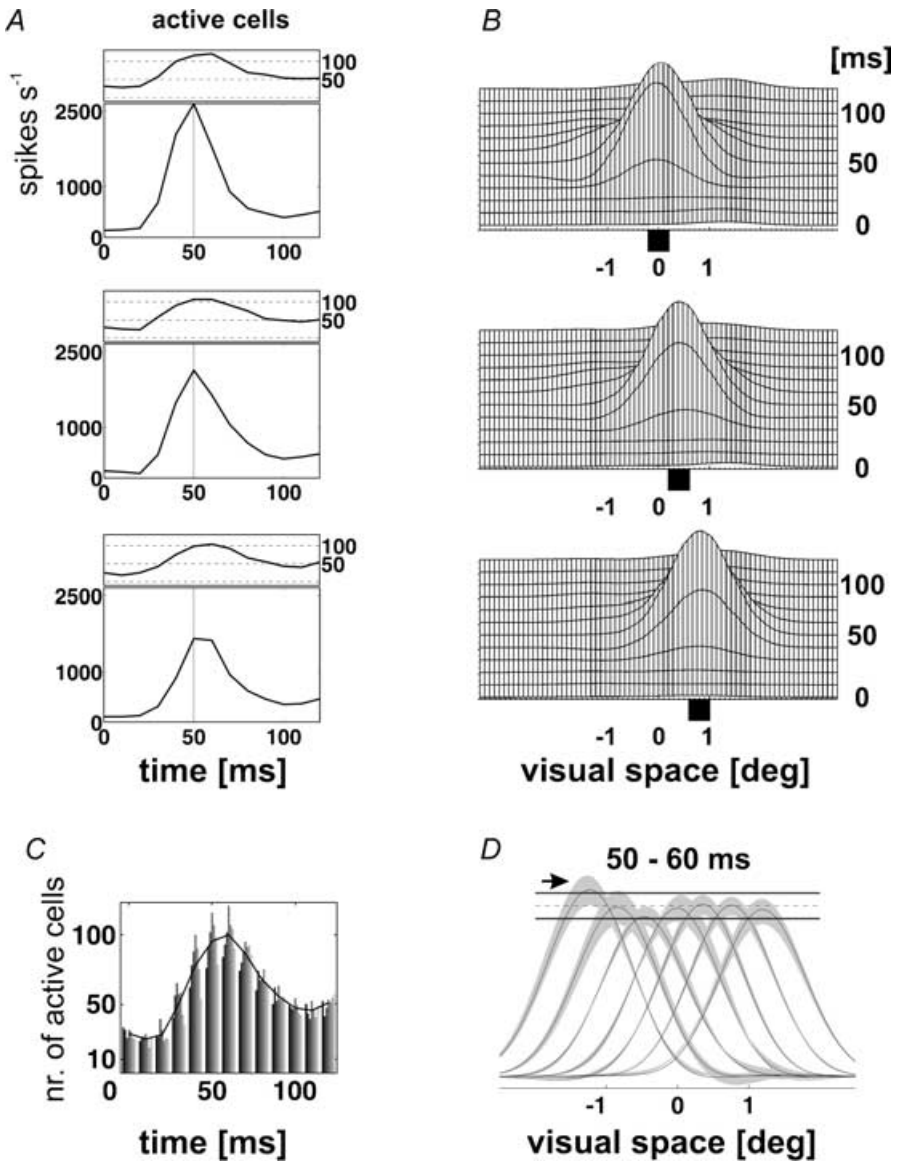

Figure 3. Population activity in response to squares flashed at different positions
A, time course of cumulative PSTHs (sum of spikes across all neurones) for squares flashed at three adjacent positions as shown in *B*. Vertical lines mark time of maximum amplitude. Upper graphs visualize the number of cells that showed significant activity ($P < 0.05$). All squares evoked similar latencies and firing rates, and involved similar numbers of cells, confirming the homogeneous sampling of visual space. *B*, space–time diagrams of OLE-derived population activity in response to the three flashed squares (black squares mark position, time on ordinate). High spatial coherence of activity within the PRF can be seen reaching its maximum centred on each stimulus position. Note that stimulus size (0.4 deg) was much smaller than the average RF size in area 17 (~2 deg, cf. Jancke *et al.* 1999). *C*, time course of the number of activated neurones in response to each of the seven squares. Single bars represent the number of responding cells within a 10 ms time bin (each bar corresponds to a given stimulus position from left (central) to right (peripheral); cf. Fig. 1*B*. At time when activity reached its maximum (50–60 ms after stimulus onset) each stimulus was represented by activity of ~90 neurones with densely overlapping RFs. *D*, bootstrap analysis. Shape and location of the PRF at time of peak maximum (50–60 ms) for all seven squares tested. A bootstrap analysis was applied to the OLE procedure (1000 iterations). Grey areas indicate 99% confidence, curves show mean. Dashed horizontal line marks the mean of the amplitudes across all flashed squares; continuous horizontal lines mark significance level ($P < 0.05$). Small fluctuations in amplitudes were of negligible significance (see arrow pointing to a slightly higher amplitude for the leftmost (central) stimulus). Each square was fairly represented by the distribution of activity centred on the respective stimulus position.

regressions of the trajectories (under the constraint of $r > 0.98$). We then measured the spatial lag between the actual maximum of the propagating peaks and the current stimulus position. Finally, for all speeds and directions, the mean spatial lag was plotted as a function of stimulus speed. As our data showed that the spatial lag increased linearly with stimulus speeds, the slope of the regression lines directly corresponds to response latency of motion (Fig. 6).

The slope of the regressions revealed latencies of 38 ms for the peripheral–central ($r = 0.99$) and 42 ms ($r = 0.99$) for central–peripheral direction. Thus the spatial lag was significantly shorter than expected from time-to-peak latencies in response to flashed stimulation (~54 ms).

In addition to speed, the spatial lag was depended on the direction of motion. For peripheral–central movements latencies were significantly smaller compared to the opposite direction, particularly for higher speeds ($P < 0.00001$ for 38.4 and 15.1 deg s^{-1}). With decreasing speed, this asymmetry became less significant due to the increasing positional scatter ($P < 0.01$ for 8.8 deg s^{-1}; $P > 0.05$ for 4.5 deg s^{-1}). For a slow speed of 4.5 deg s^{-1}, the reduced latency for peripheral–central motion led to a match between the peak of population activity and actual stimulus position as indicated by a spatial lag of nearly zero.

Discussion

We showed that in cat primary visual cortex small moving squares of light can be represented as propagating peaks of activity across a 'population receptive field'. Latencies for motion were significantly shorter than expected from the response to flashed stimuli, indicating reduced neural processing times. For slow peripheral–central movements (4.5 deg s^{-1}) we observed compensation of neural latencies. At higher speeds and for motion in the opposite direction, we found a spatial lag between the moving stimulus and its representing peak of population activity. This spatial lag increased with increasing stimulus speeds.

On the single cell level, neural latencies have been shown to vary within a wide range of delay times. Generally, neurones that were sensitive to high stimulus speeds were also found to have short latencies for stationary light bars (Duysens *et al.* 1982). Comparing responses to flashed and moving slits of light, only a few cells showed reduced latencies (Bishop *et al.* 1971). A stimulus dark edge evoked responses in advance of the discharge coming from the stimulus light edge (Bishop *et al.* 1971, 1973). Also, LGN neurones were found to respond

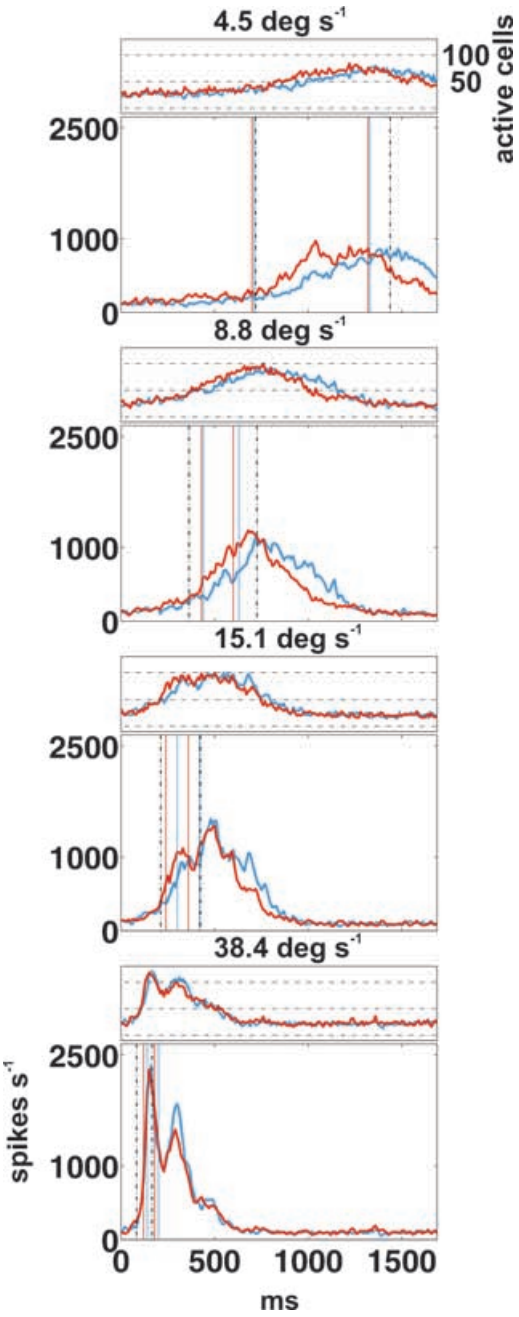

Figure 4. Sum of spike rates (cumulative PSTHs) in response to squares moving at different speeds
Motion in centro-peripheral direction is outlined in blue, red curves depict peripheral–central direction (speeds indicated on top). Overall activity increased with increasing stimulus speeds. Vertical interrupted lines show point in time when the stimulus entered and left the sampled space; vertical red and blue lines mark time period in which significant propagation of activity was observed when applying the OLE procedure (cf. Fig. 5). Upper graphs show number of cells significantly active within each 10 ms time step. Note that similar numbers of neurones were activated for all stimulus speeds.

with shorter delays to moving than for flashed light bars (Orban *et al.* 1985). Some of these controversial findings may result from the relatively wide bin sizes used for analysis, which makes it difficult to detect small changes in latencies at the single cell level. Furthermore, the spatial-lag method is critically sensitive to response variability of single cells. The population approach used here, however, transforms the various spatio-temporal dynamics of single cell activity into homogeneous activity patterns at the population level (Dinse & Jancke, 2001*a*), indicating a qualitative difference between microscopic and mesoscopic processing levels (Freeman, 2000). As a consequence, the population approach permits the dense and fine-scaled analysis of activity trajectories across a representative neural population.

Motion anticipation in V1: a novel achievement in the representation of stimulus position?

Judging correctly the location of moving objects is of crucial importance for evading obstacles or predators or for catching prey. This task would be almost impossible, particularly for high speeds, if the relevant information is delayed due to neural conduction and processing times. To overcome this problem, compensatory mechanisms have evolved that allow for anticipation of the path of motion.

Recently, it has been demonstrated that already at the retinal level a population of ganglion cells provides a first step in the generation of anticipatory processes (Berry *et al.* 1999). These authors showed that a non-linear

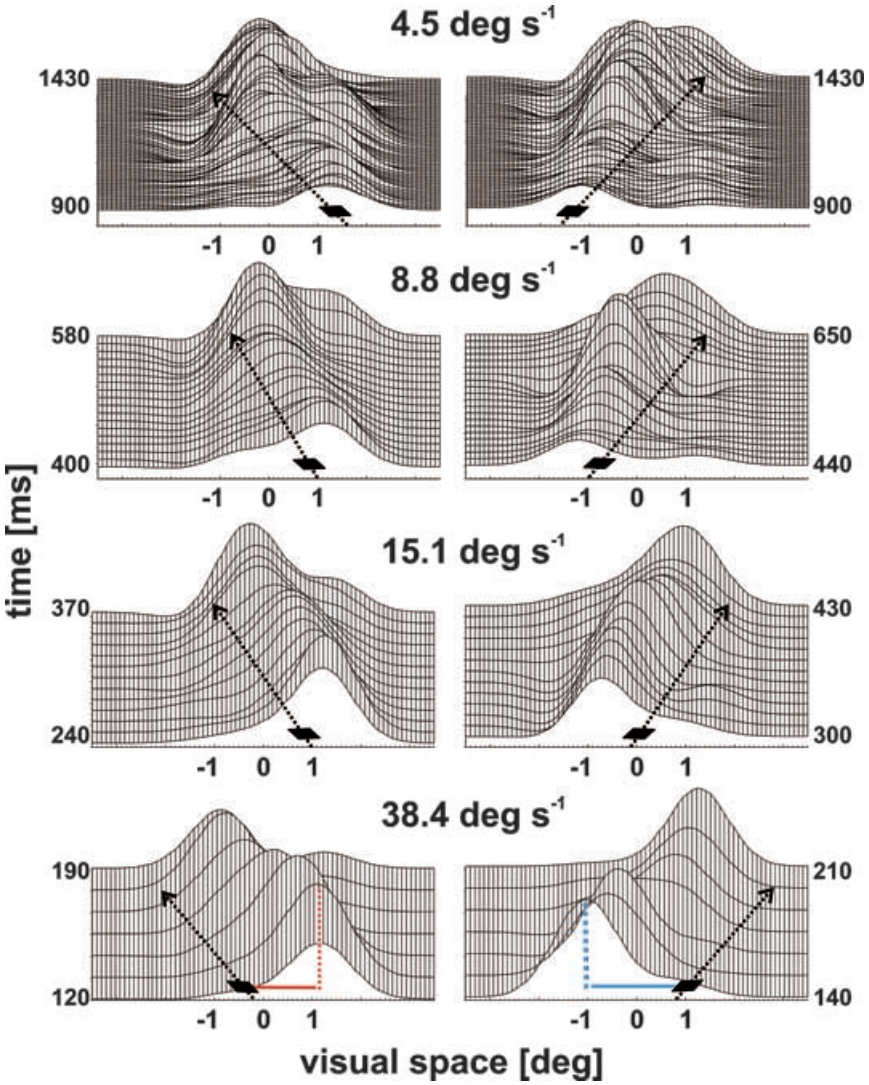

Figure 5. Motion trajectories across the population receptive field (PRF)
Space–time diagrams of activity representing squares (shown in black) that moved with different speeds and directions; arrows indicate stimulus trajectories. Profiles were derived by OLE. *x*-axis depicts visual space in degrees, with zero indicating midpoint of trajectories. Starting position of movement was at ± 3.2 deg. The *y*-axis resolves 10 ms time steps within the time interval in which propagation of activity occurred. Activity was normalized for each speed separately. The different tilt angles of the space–time plots arise from activity peaks matching stimulus speed and direction. Red and blue lines in the bottom row sketch the spatial lag between current stimulus position and peak location within the PRF.

contrast-gain control mechanism, together with spatially extended receptive fields and a biphasic temporal response, are prerequisites to accounting for the observed effects. Translating their data from millimetres of retina into visual field coordinates (cf. Hughes, 1971; DeVries & Baylor, 1997), the retinal compensatory mechanisms was limited to stimulus speeds of approximately 5 deg s^{-1} which is in accordance with our result for peripheral–central motion direction. While we found a reduction of latencies up to 40 deg s^{-1}, latencies for this range of speeds have not been investigated at the retinal level.

Directional asymmetry

In addition to the retinal data, our cortical data showed that the reduction of latencies to moving stimuli depends on direction of motion. Directional asymmetries guiding the optokinetic reflex have recently been found in monkey areas V5/V5+ (Hoffmann *et al.* 2002) as well as for position judgement tasks in human subjects (Müsseler & Aschersleben, 1998): A small visual target which moves in the peripheral–central direction is perceived with a latency shorter than for the same target moving away from the fovea (Mateeff & Hohnsbein, 1988; Mateeff *et al.* 1991*a*,*b*). Single object motion, as applied in our study, may predominantly stimulate the so-called displacement-analysing system preferring foveopetal motion (opposed to a motion-analysing system that encodes 'en masse' dot motion; Bonnet, 1984). Such a system was speculated to emphasize motion towards a centrally fixed target (Mateeff *et al.* 1991*a*).

Spatial asymmetries for representations of moving objects might be the result of active mechanisms compensating neural delays for one direction on the cost of longer delays in the opposite direction (Jensen & Martin, 1980). van Beers *et al.* (2001) proposed a number of putative mechanisms underlying differences in localization for foveopetal and foveofugal motion. These mechanisms include temporal asymmetries in neural delays, and a partial asymmetric spatial expansion of the retinal representation, both comparable to our findings. On the other hand, these authors provided evidence that when shifting gaze, the central nervous system is able to compensate for localization errors by sensorimotor integration to maintain position constancy, maybe by taking advantage of these internally generated erroneous position signals.

Cellular mechanisms of preactivation

Long-range horizontal connections may constitute a possible substrate for preactivation as spreading subthreshold activity (Grinvald *et al.* 1994; Bringuier *et al.* 1999) extends far beyond the classical RF (Allman *et al.* 1985). Applying voltage-sensitive dye optical imaging in cat area 18, a method that emphasizes subthreshold synaptic potentials (Grinvald *et al.* 1994), we recently showed propagating waves of subthreshold activity in response to moving squares that covered large cortical regions ahead in time of the thalamic input (Jancke *et al.* 2004). In addition, using intracellular recordings in combination with a priming stimulus, reduced cortical latencies in the range reported here have been shown for subthreshold response components (Hirsch *et al.* 1998).

Extracellular recordings as employed in our study provide no information about the accompanying intracellular events. As a possible mechanism we suggest that preactivation resulting from preceding stimulus displacements along the trajectory lead to an increased probability of firing action potentials when the stimulus moves across the PRF. In terms of spike rates of single cell RFs, such behaviour would cause an asymmetric

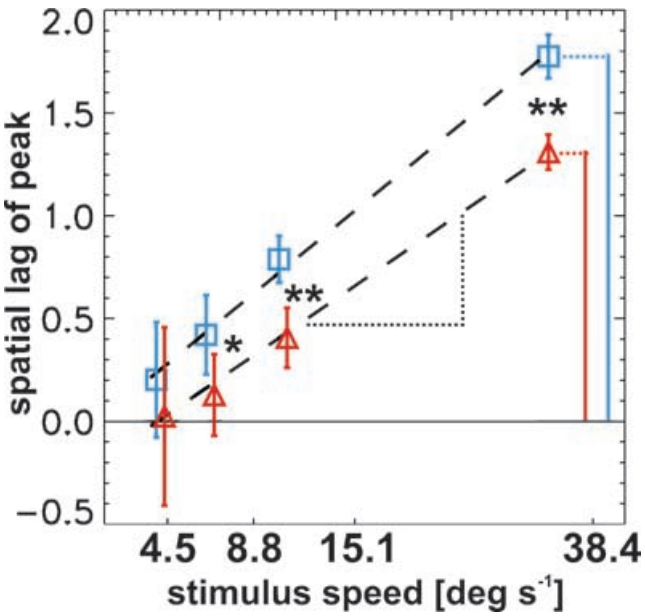

Figure 6. Calculation of latencies for moving stimuli: speed dependence of the spatial lag
The average spatial lag between the peak of population activity and the actual position of the moving stimulus increased with stimulus speeds. Data points show mean spatial lags for each speed and direction (bootstrap, $n = 1000$). Blue squares indicate centro-peripheral movement, red triangles indicate opposite direction (vertical blue and red lines sketch spatial lags for a speed of 38.4 deg s^{-1} as shown in Fig. 4, bottom). Latencies were calculated by linear regression. Latency was 42 ms for centro-peripheral motion and 38 ms for peripheral-central direction. Significance of direction difference: $^{**}P < 0.00001$; $^{*}P < 0.01$.

enlargement of RF sizes. As a consequence, RFs are shifted in the motion direction, causing neurones to respond with shorter latencies. Likewise, one might interpret such a shift as a primarily spatial phenomenon: RF boundaries that were not responsive when mapped with flashed stimuli, become responsive when a stimulus moves, and RFs are therefore 'pulled' towards a moving stimulus (Pulgarin *et al.* 2003).

Latency differences may contribute to the flash-lag effect

There is an extensive ongoing discussion about the nature of the psychophysically observed flash-lag effect (FLE), which has been studied under a large variety of experimental designs (Metzger, 1932; MacKay, 1958; Nijhawan, 1994; Purushothaman *et al.* 1998; Krekelberg & Lappe, 1999; Kirschfeld & Kammer, 1999; Eagleman & Sejnowski, 2000; Krekelberg *et al.* 2000; Sheth *et al.* 2000; Whitney *et al.* 2000; Krekelberg & Lappe, 2001). However, the neural substrates underlying this effect remain unknown.

The FLE has also been reported with no retinal motion, indicating that extra-retinal information can be used to derive alternative motion information (Schlag *et al.* 2000). Moreover, the FLE phenomenon not only applies to motion, but to other dimensions as well, such as colour (Sheth *et al.* 2000). However, while not designed to mimic a particular psychophysical experiment – our experimental set-up corresponds to the traditional continuous motion protocol (Hazelhoff & Wiersma, 1924) – the presented data revealed a ∼16 ms difference in latency between a flash and a moving stimulus, corresponding to a 30% reduction in processing time when the stimulus moves. For the FLE described by Eagleman & Sejnowski (2000), the stimulus moved at 360 deg s^{-1} rotation angle, leading to a displacement of about 5 deg, which translates into a delay of 14 ms and is thus within the same range as found in our study. On the other hand, latency differences obtained in various FLE paradigms commonly range between 40 and 80 ms (Krekelberg & Lappe, 2001), most probably involving additional mechanisms in downstream cortical areas. Furthermore, compensation for neural processing times must not necessarily be restricted to the perceptual domain. It has recently been demonstrated that pointing movements towards the final position of a moving target were directed beyond its vanishing point, suggesting that for goal-directed tasks, sensorimotor integration is critical for compensation of neural latencies (Kerzel & Gegenfurtner, 2003).

However, vision is not exclusively involved in the processing of time-critical stimulus characteristics. In an earlier study we reported that after the horizontally moving square has passed the PRF, population activity was smeared out in space, producing a motion streak (Jancke, 2000). Subsequent to positional coding, this later part of the response (cf. Fig. 4) contained information about the orientation of the stimulus trajectory, i.e. activation was dominated by neurones tuned to horizontal orientation. This suggests that the primary visual cortex codes orientation by integrating past stimulus positions and thus conveys different stimulus aspects in different moments in time.

There is still not much knowledge about how timing information provided by visual cortical neurones maps to perception. Along the visual pathway various predictive (Nijhawan, 1994; Rao & Ballard, 1999) and integrative mechanisms (Krekelberg & Lappe, 1999; Eagleman & Sejnowski, 2000), from mechanisms in the retina (Berry *et al.* 1999) through to sensorimotor transformation mechanisms (Kerzel & Gegenfurtner, 2003), are involved in motion processing. It remains an open question how the representation of moving stimuli in primary visual cortex, in particular its reduced response latencies as reported here, contribute to the processing of object position in the higher brain.

References

Allman J, Miezin F & McGuiness E (1985). Stimulus specific responses from beyond the classical receptive field: neurophysiological mechanisms for local-global comparisons in visual neurons. *Annu Rev Neurosci* **8**, 407–430.

Anderson CH (1994). Basic elements of biological computional systems. *Int J Modern Physics C* **5**, 135–137.

Berry MJ II, Brivanlou IH, Jordan TA & Meister M (1999). Anticipation of moving stimuli by the retina. *Nature* **398**, 334–338.

Bishop PO, Coombs JS & Henry GH (1971). Responses to visual contours: Spatio-temporal aspects of excitation in the receptive fields of simple striate neurones. *J Physiol* **219**, 625–657.

Bishop PO, Coombs JS & Henry GH (1973). Receptive fields of simple cells in the cat striate cortex. *J Physiol* **231**, 31–60.

Bonnet C (1984). Two systems in the detection of visual motion. *Ophthalmic Physiol Opt* **4**, 61–65.

Bringuier V, Chavane F, Glaeser L & Frégnac Y (1999). Horizontal propagation of visual activity in the synaptic integration field of area 17 neurons. *Science* **283**, 695–699.

Camarda RM, Peterhans E & Bishop PO (1985). Simple cells in cat striate cortex: responses to stationary flashing and to moving light bars. *Exp Brain Res* **60**, 151–158.

Dayan P & Abbott LF (2001). *Theoretical Neuroscience: Computational and Mathematical Modeling of Neural Systems*. MIT Press, Cambridge, MA, USA.

DeVries SH & Baylor DA (1997). Mosaic arrangement of ganglion cell receptive fields in rabbit retina. *J Neurophysiol* **78**, 2048–2060.

Dinse HR & Jancke D (2001*a*). Time-variant processing in V1: From microscopic (single cell) to mesoscopic (population) levels. *Trends Neurosci* **24**, 203–205.

Dinse HR & Jancke D (2001*b*). Comparative population analysis of cortical representations in parametric spaces of visual field and skin: a unifying role for nonlinear interactions as a basis for active information processing across modalities. *Prog Brain Res* **130**, 155–173.

Duysens J, Orban GA & Verbeke O (1982). Velocity sensitivity mechanisms in cat visual cortex. *Exp Brain Res* **45**, 285–294.

Eagleman DM & Sejnowski TJ (2000). Motion integration and postdiction in visual awareness. *Science* **287**, 2036–2038.

Erlhagen W, Bastian A, Jancke D, Riehle A & Schöner G (1999). The distribution of neuronal population activation (DPA) as a tool to study interaction and integration in cortical representations. *J Neurosci Meth* **94**, 53–66.

Fitzpatrick D (2000). Seeing beyond the receptive field in primary visual cortex. *Curr Opin Neurobiol* **10**, 438–443.

Freeman WJ (2000). Mesoscopic neurodynamics: from neuron to brain. *J Physiol (Paris)* **94**, 303–322.

Gegenfurtner KR & Hawken MJ (1996). Interaction of motion and color in the visual pathways. *TINS* **19**, 394–400.

Grinvald A, Lieke E, Frostig R & Hildesheim R (1994). Real-time optical imaging of naturally evoked electrical activity in intact frog brain. *J Neurosci* **14**, 2545–2568.

Hazelhoff FF & Wiersma H (1924). Die Wahrnehmungszeit [The sensation time]. *Z Psychologie* **96**, 171–188.

Hirsch JA, Alonso JM, Reid RC & Martinez LM (1998). Synaptic integration in striate cortical simple cells. *J Neurosci* **18**, 9517–9528.

Hoffmann KP, Bremmer F, Thiele A & Distler C (2002). Directional asymmetry of neurons in cortical areas MT and MST projecting to the NOT-DTN in macaques. *J Neurophysiol* **87**, 2113–2123.

Hughes A (1971). Topographical relationships between the anatomy and physiology of the rabbit visual system. *Doc Ophthalmol* **30**, 33–159.

Jancke D (2000). Orientation formed by a spot's trajectory: A two-dimensional population approach in primary visual cortex. *J Neurosci* **20**, RC86, 1–6.

Jancke D, Akhavan AC, Erlhagen W, Schöner G & Dinse HR (1996). Reconstruction of motion trajectories from the dynamic population representation of neurons in cat visual cortex. *Soc Neurosci Abstract* **22**, 646.

Jancke D, Chavane F, Naaman S & Grinvald A (2004). Imaging correlates of visual illusion in early visual cortex. *Nature* **428**, 423–426.

Jancke D, Erlhagen W, Dinse HR, Akhavan AC, Giese M, Steinhage A & Schöner G (1999). Parametric population representation of retinal location: Neuronal interaction dynamics in cat primary visual cortex. *J Neurosci* **19**, 9016–9028.

Jensen HJ & Martin J (1980). On localization of moving objects in the visual system of cats. *Biol Cybern* **36**, 173–177.

Kerzel D & Gegenfurtner KR (2003). Neuronal processing delays are compensated in the sensorimotor branch of the visual system. *Curr Biol* **13**, 1975–1978.

Kirschfeld K & Kammer T (1999). The Fröhlich effect: a consequence of the interaction of visual focal attention and metacontrast. *Vision Res* **39**, 3702–3709.

Krekelberg B & Lappe M (1999). Temporal recruitment along the trajectory of moving objects and the perception of position. *Vision Res* **39**, 2669–2679.

Krekelberg B & Lappe M (2001). Neuronal latencies and the position of moving objects. *Trends Neurosci* **24**, 335–339.

Krekelberg B, Lappe M, Whitney D, Cavanagh P, Eagleman DM & Sejnowski TJ (2000). The position of moving objects. *Science* **289**, 1107a.

MacKay DM (1958). Perceptual stability of a stroboscopically lit visual field containing self-luminous objects. *Nature* **181**, 507–508.

Mateeff S, Bohdanecky Z, Hohnsbein J, Ehrenstein WH & Yakimoff N (1991*b*). A constant latency difference determines directional anisotropy in visual motion perception. *Vision Res* **31**, 2235–2237.

Mateeff S & Hohnsbein J (1988). Percepual latencies are shorter for motion towards the fovea than for motion away. *Vision Res* **28**, 711–719.

Mateeff S, Yakimoff N, Hohnsbein J, Ehrenstein WH, Bohdanecky Z & Radil T (1991*a*). Selective directional sensitivity in visual motion perception. *Vision Res* **31**, 131–138.

Metzger W (1932). Versuch einer gemeinsamen Theorie der Phänomene Fröhlichs und Hazelhoffs und Kritik ihrer Verfahren zur Messung der Empfindungszeit. *Psychol Forsch* **16**, 176–200.

Müsseler J & Aschersleben G (1998). Localizing the first position of a moving stimulus: The Fröhlich effect and an attention-shifting explanation. *Perception Psychophysics* **60**, 683–695.

Nicolelis MA, Ghazanfar AA, Stambaugh CR, Oliveira LM, Laubach M, Chapin JK, Nelson RJ & Kaas JH (1998). Simultaneous encoding of tactile information by three primate cortical areas. *Nat Neurosci* **1**, 621–630.

Nijhawan R (1994). Motion extrapolation in catching. *Nature* **370**, 256–257.

Orban GA (1984). Neuronal operations in the visual cortex. In *Studies of Brain Function XI*, ed. Braitenberg, V., pp. 1–367. Springer, New York.

Orban GA, Hoffmann KP & Duysens J (1985). Velocity selectivity in the cat visual system. I. Responses of LGN cells to moving bar stimuli: a comparison with cortical areas 17 and 18. *J Neurophysiol* **54**, 1026–1049.

Pulgarin M, Nevado A, Guo K, Robertson RG, Thiele A & Young MP (2003). Spatio-temporal regularities beyond the classical receptive field affect the information conveyed by the responses of V1 neurons. *Soc Neurosci Abstract* **33**, 910.16.

Purushothaman G, Patel SS, Bedell HE & Ogmen H (1998). Moving ahead through differential visual latency. *Nature* **396**, 424.

Rao RPN & Ballard DH (1999). Predictive coding in the visual cortex: a functional interpretation of some extra-classical receptive field effects. *Nat Neurosci* **2**, 79–87.

Salinas E & Abbott LF (1994). Vector reconstruction from firing rates. *J Comput Neurosci* **1**, 89–107.

Schlag J, Cai RH, Dorfman A, Mohempour A & Schlag-Rey M (2000). Extrapolating movement without retinal motion. *Nature* **403**, 38–39.

Sheth BR, Nijhawan R & Shimojo S (2000). Changing objects lead briefly flashed ones. *Nat Neurosci* **3**, 489–495.

Szulborski RG & Palmer LA (1990). The two-dimensional spatial structure of nonlinear subunits in the RFs of complex cells. *Vision Res* **30**, 249–254.

Whitney D, Murakami I & Cavanagh P (2000). Illusory spatial offset of a flash relative to a moving stimulus is caused by differential latencies for moving and flashed stimuli. *Vision Res* **40**, 137–149.

van Beers RJ, Wolpert DM & Haggard P (2001). Sensorimotor integration compensates for visual localization errors during smooth pursuit eye movements. *J Neurophysiol* **85**, 1914–1922.

Acknowledgements

We thank Dr Axel Steinhage for implementation of the OLE in MATLAB©, Drs W. von Seelen, K.-P. Hoffmann for helpful discussion, and Drs A. Arieli, K. Kirschfeld, C. Schreiner, H. Wagner, F. Chavane, and Y. Frégnac for critical and constructive comments on earlier versions of the manuscript. The work was supported by grants from the Deutsche Forschungsgemeinschaft (Scho 336/4-2 and Di 334/5-1,3).

Supplementary material

The online version of this paper can be found at:

DOI: 10.1113/jphysiol.2003.058941

and contains supplementary material entitled:

Bootstrap analysis. This material can also be accessed at http://www.blackwellpublishing.com/products/journals/suppmat/tjp/tjp217/tjp217sm.htm